Relation between incommensurate modulation and Tc in Bi-Sr-Ca-Cu-O superconductors

Z.C. Kang, O. Monnereau, F. Remy, S. Spas, A. Casalot, J.P. Sorbier, A. Fournel, C. Boulesteix

Classification
Physics Abstracts
61.14 — 74.10 — 74.70

Relation between incommensurate modulation and T_c in Bi-Sr-Ca-Cu-O superconductors

Z. C. Kang (*), (**), O. Monnereau (**), F. Remy (**), S. Spas (**), A. Casalot (**), J. P. Sorbier (***), A. Fournel (***) and C. Boulesteix (*)

(*) Lab. de Microscopie Electronique Appliquée, Case B61, Faculté des Sciences de St-Jérôme. 13397 Marseille Cedex 13, France
(**) Lab. de Chimie des Matériaux, Université de Provence, Case 26, 3 place Victor-Hugo, 13331 Marseille Cedex 3, France
(***) Lab. d'Electronique des Milieux Condensés, Faculté des Sciences de St-Jérôme, 13397 Marseille Cedex 13, France

(*Reçu le 21 novembre 1988, révisé le 28 décembre 1988, accepté le 24 janvier 1989*)

Résumé. — Des échantillons de la composition normale (2212) ont été recuits at 880, 904, 925, 940 et 950 °C, puis refroidis jusqu'à l'ambiante à la vitesse de 2°/heure pour obtenir de petits monocristaux. La résistivité de ces échantillons a été mesurée. La température de transition supraconductrice T_c est la plus basse (86 K) pour la plus basse température de recuit et la plus élevée pour la plus haute température de recuit (94 K). Les échantillons été été caractérisés par microanalyse et microdiffraction. Une modulation incommensurable se produit toujours le long (ou très près de la direction) de $\mathbf{b}^*$, avec différentes valeurs de $\mathbf{q}^*$ ($\mathbf{q}^* = 2\,\mathbf{b}^*/4{,}80$, $\mathbf{q}^* = 2\,\mathbf{b}/9{,}89$). La modulation de la phase incommensurable pour laquelle $T_c = 94$ K et dont la composition est la composition standard (2212) est approximativement sinusoïdale avec un seul satellite, et les phases incommensurables dans la région non sinusoïdale, avec plusieurs satellites ont des valeurs de $2\,b^*/q^*$ proches de l'entier 10, avec des écarts de composition relative pour les cations Sr, Ca, et Bi, et une valeur T_c plus basse (86 K). On compare ces résultats avec des résultats antérieurs.

Abstract. — Samples of the normal composition (2212) have been heated to 880, 904, 925, 940 and 950 °C, then cooled at 2 °C/Hour to obtain small single crystals. The resistivity of these samples was measured. T_c is lowest (86 K) for the lowest treatment temperature and highest (94 K) for the highest treatment temperature. The samples have been characterized by microanalysis and microdiffraction. An incommensurate modulation always occurs along (or close to) $\mathbf{b}^*$ with different possible $\mathbf{q}^*$ values ($\mathbf{q}^* = 2\,\mathbf{b}^*/4.80$, $\mathbf{q}^* = 2\,\mathbf{b}/9.89$). The incommensurate phase, with $T_c = 94$ K and standard (2212) composition, is approximately sinuoisdal with only one satellite. The incommensurate phases in the unsinusoidal region, with several harmonic satellites, have $2\,b^*/q^*$ values close to integer 10, a composition ratio deviation for the Sr, Ca, and Bi cation, and a lower T_c (86 K). A comparison with previous results has been performed.

Introduction.

Since the high T_c superconductor based on the Bi-Sr-Ca-Cu-O system was prepared [1], a lot of articles, concerning the superconducting phases investigated by electron microscopy, have been published. The so-called (2212) and (2223) phases, with short and long periods along the **c** axis respectively, are probably related to the low T_c and high T_c values as shown by [2]. Imperfect stacking with mixed phases has also been revealed by high resolution electron microscopy [2]. This fact is a common phenomenon for the Aurivillius family $(Bi_2O_2)^{+2}(A_{n-1}B_nO_{3n+1})$ compounds [3]. An incommensurate modulation along (or close to) the **b*** axis has been shown in the diffraction pattern in most articles [2, 4 to 14]. Recently, the lattice displacement of the modulation at the atomic scale has been clearly presented [7, 8]. This modulation has also been observed in X-ray diffraction patterns and all the extra peaks can be indexed by four integer indices $\mathbf{G}^* = h\mathbf{a}^* + k\mathbf{b}^* + \ell\mathbf{c}^* + m\mathbf{q}^*$, where $\mathbf{q}^*$ is the modulation wave vector [12]. However, the modulation in the superconducting phases is still a puzzling problem. X-ray powder diffraction patterns of two compounds, with 85 K and 110 K T_c values respectively, do not indicate noticeable changes having only differences in extra peaks [15]. This fact implies that the difference between the low and high T_c phases could be related to the modulation. Kijima *et al.* [6], using analytical electron microscopy combining EDX and diffraction, recently indicated that the 105 K and 75 K superconducting phases have the same structure but with some atomic disordering and atomic deficiencies. Matsui *et al.* [8], using EDX analysis and microdiffraction (a technique previously used by Bando *et al.* [5]), showed the existence of two types of modulation in both low (75 K) and high (105 K) T_c phases. The $Tl_2Ba_2CaCu_2O_{8+y}$ (2212) type phases (so-called low T_c phases) are not, or very faintly, modulated, they have a T_c up to 120 K [16].

As Tarascon *et al.* [15] pointed out, heat treating (4334) compounds (very close to, but not above their melting point) generates a material with a T_c of 110 K and the critical transition temperature is sensitive to this high temperature treatment. Of course, there are other problems with the composition of these phases. The measured composition, for example, corresponding to regions where the diffraction patterns were made, has shown a wide composition range, Ca-poor (or Sr-enriched) regions, by EDX analysis [6].

To our knowledge no report combining T_c temperature, composition, and diffraction of a single specimen has been published yet. Using analytical electron microscopy on samples where the resistivity had been measured *versus* temperature, we attempted to relate microdiffraction to composition for the same area, and found two types of modulation corresponding to two different compositions : Ca-poor and Ca-rich in both (2212) type ceramics and single crystals. In this report we will show the relationship between modulation, T_c temperature, and high temperature treatment of single crystal samples. From these data, we will discuss the nature of incommensurate superconducting phases.

Review of data on diffraction patterns in the ⟨001⟩ zone.

A lot of electron diffraction patterns in the ⟨001⟩ zone have been published. They have some similarities but also some real differences. In the interest of clarity we have put them in a table (table I).

As indicated by [17], four different kinds of reflections, referring to perovskite sublattice, can be distinguished (Fig. 1a) : **A** spots (corresponding to 2 **a*** or 2 **b*** in the indexation of the generally accepted structure of the compound), which are the main reflections with the strongest intensity, corresponding to the 110 type reflections of the perovskite lattice with a periodicity of 2.7 Å in real space. They are indexed as $2(h\mathbf{a}^* + k\mathbf{b}^*)$. **B** spots, a series of spots

Table I. — *Published diffraction patterns of modulated structures.*

Authors	B spots	C spots	D spots	$m = 1$	$m = 2$	T_c	Treatment T	Expected Composition
Bando Y. [5]	nv	nv	nv	w	s	70 K	820 °C	$Bi_2(SrCa)_2Cu_2O_y$
Kijima T. [6]	nv	nv	nv	nv	s	75 K	850 °C	$Bi_2(SrCa)_4Cu_2O_y$
Matsui Y. [7]	nv	nv	nv	nv	s	105 K	882 °C	$Bi_4(Sr_3Ca)_3Cu_6O_y$
Matsui Y. [8]a*	nv	nv	nv	nv	s	70 K	800 °C	$Bi_4(Sr_3Ca)_2Cu_6O_y$
Matsui Y. [8] b*	m	v	nv	s	m			
Hiraga K. [9]	nv	nv	nv	nv	s	75-110 K	800-850 °C	
Takayama E. [10]	m	ww	nv	s	m	80 K	700-900 °C	$Bi_4(Sr_3Ca)_3Cu_4O_y$
Kijima N. [11]	v	nv	nv	m	m	80-107 K	870 °C	$Bi(SrCa)_3Cu_4O_y$
Onoda [12]	nv	nv	nv	w	s		850 °C	$Bi_4(Sr_3Ca)_3Cu_4O_y$
Tollon [13]	m	v	v	s	s	91 K	830-870 °C	
van Tendeloo a**	nv	nv	nv	w	s			
[2] b**	v	nv	v	w	s			
[4]	m	nv	nv	s	w			
Subramaniam [14]	nv	nv	nv	s	w		700-900 °C	

* Fig. 2a and 2b of 8].
** [Fig. 1c and 4d of 2].
nv = non visible, v = visible, vw = very weak, w = weak, m = medium, s = strong.

with medium intensity, corresponding to a periodicity of 5.4 Å in real space and related to a superstructure of the perovskite sublattice in the $[1\bar{1}0]$ direction of the perovskite sublattice. They are indexed as $(2h + 1)\,\mathbf{a}^* + 2k\mathbf{b}^*$. **C** spots, a series of spots with still weaker intensity located at the center of squares of main reflections. They correspond to the $\langle 100 \rangle$ type reflections of the perovskite sublattice and are indexed as $(2h + 1)\,\mathbf{a}^* + (2k + 1)\,\mathbf{b}^*$. **D** spots, in the [110] direction of the perovskite sublattice, similar to **B** spots but perpendicular to them and indexed as $2h\mathbf{a}^* + (2k + 1)\,\mathbf{b}^*$. Any reflection vector **G*** can be indexed with four indices :

$$\mathbf{G}^* = h\mathbf{a}^* + k\mathbf{b}^* + \ell\mathbf{c}^* + m\mathbf{q}^*$$

where $\mathbf{q}^*$ is the modulation wave vector parallel (or very close) to $\mathbf{b}^*$; m being the index of modulation satellites.

In table I we have listed the intensity of the diffraction spots in the $\langle 001 \rangle$ zone as appearing in the literature. For a comparison of the data we have also indicated the expected or measured composition, the T_c temperature, and the heat treatment temperature. In this table the indication *non visible* may be *very weak* (because we got it from published prints) but the intensity differences can be clearly distinguished. To compare the intensity of spots a correct orientation of the crystal should be necessary, so that same kind of spots have same intensity ; in some papers this is only approximatively true, and could be the origin of small errors.

From listed data we can see that there are three types of diffraction patterns : the first type (called M_1, Fig. 1b) : $m = 1$ is weak (or non visible on the print) but $m = 2$ is strong, then the **B**, **C**, **D** spots are non visible ; the second type (called M_2, Fig. 1c) : $m = 1$ is strong and $m = 2$ is weak, then **B** are medium, **C** are very weak, **D** are non visible ; the third type (called M_3, Fig. 1d) : $m = 1, 2$ are medium, then **B**, **C**, **D** are visible. The M_1 type occurs for samples heated up to 850 °C, M_2 for samples heated to less than 850 °C, M_3 for samples heated up to

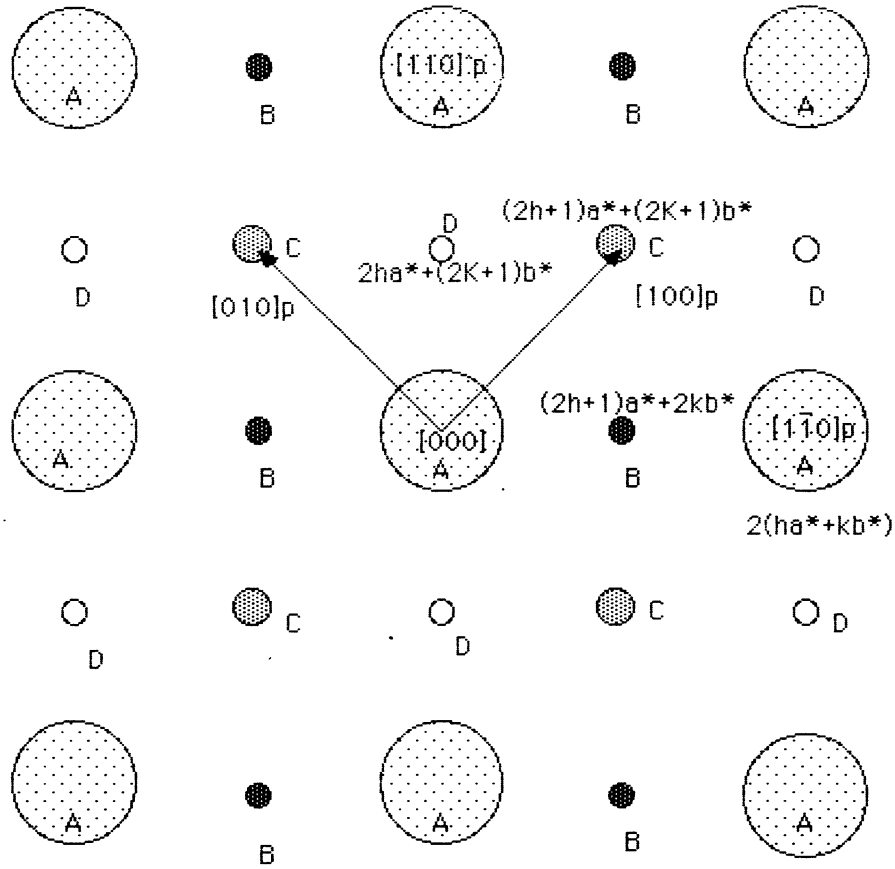

Fig. 1a. — In the standard diffraction pattern of a perovskite structure **B** and **D** spots are equivalent. It is not the case for the Bi superconductors.

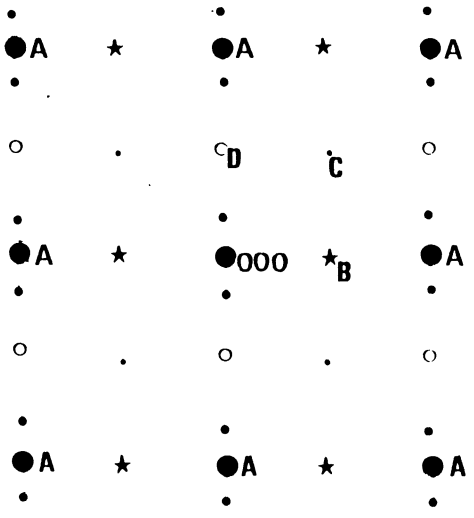

b) Diffraction pattern for the M_1 type.

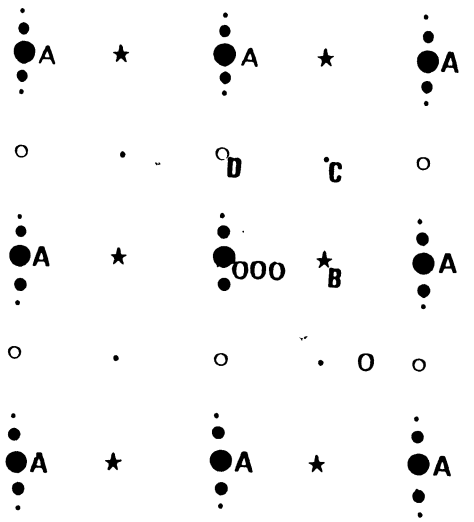

c) Diffraction pattern for the M_2 type.

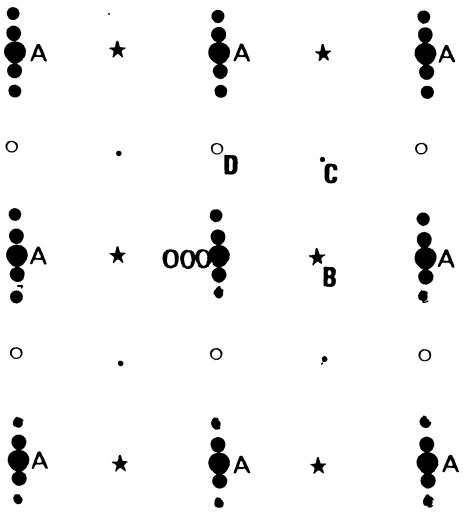

d) Diffraction pattern for the M_3 type.

Note :

●	--- A type spots	*	--- stronger satellite spots
□	--- B type spots	○	--- weaker satellite spots
△	--- C type spots	+	--- invisible satellite spots
▭	--- D type spots		

870 °C. Only Mastsui [8] indicated the existence of two types of diffraction patterns in both low and hight T_c samples, but there was no discussion. The T_c temperature and composition from different authors are hard to compare.

In previous results of our group [17] two cases occurred in ceramic samples. First : $m = 1$ satellites are strong, $m = 2$ weak, and **B** spots are strong, **C** are medium, and **D** are invisible. Satellites around **B** spots are absent or very weak. This situation is very similar to the M_2 type. Crystallites are generally needle-like and Ca-poor. The q^* value is $2\,b^*/9.45$.

Second : $m = 1, 2$ are medium with nearly the same intensity, **B** spots are medium, **C** are weak, and **D** are very weak. This situation is very similar to the M_3 type. The crystallites are plate-like and Ca-rich ([Sr]/[Ca] close to 2). The q^* value is $2\,b^*/9.9$ (close to 10, but different, as can be seen from the distance between satellites).

From the point of view of incommensurate phase transitions the M_1 and M_2 modulation types, with only one strong satellite, are mainly sinusoidal modulations and should correspond to a phase far from a possible lock-in transition. The M_3 type modulation should correspond to a phase inside the unsinusoidal (or multisoliton) region because it is far from a sinusoidal modulation. We believe that for our ceramic sample, the first case is an incommensurate phase with approximate sinusoidal modulation, and second one is an incommesurate phase in the unsinusoidal region.

Experimental results on relationship between modulation type, treatment temperature and T_c.

Using standard methods, we prepared a sample having the normal (2212) composition. Samples are synthetized from calcium (4N5) and strontium (4N5) carbonates, copper (5N)

and bismuth (5N) oxides. Powders are weighed in such quantities to correspond to the normal (2212) composition. They are carefully crushed together and are submitted to a first heat treatment at 800° for at least 12 hours, inside a gold crucible. They are crushed again, compacted and submitted to a new heat treatment at 850° (± 10°) for a few days. Samples are then taken for few hours at a temperature that could vary from 880° to 950° (± 5°), close or even above the melting point. They are slowly cooled (2°/Hour) to 770°, then the electric power is turned off, the sample being maintained inside the furnace and cooled to room temperature. This gives rise to the formation of small crystals with facets extending until about one millimeter. Five of these crystals have been selected for further studies, treatment temperatures for them were respectively : No. 1 : 880 °C ; No. 2 : 904 °C ; No. 3 : 925 °C ; No. 4 : 940 °C ; No. 5 : 950°C. For each of them resistivity was measured *versus* temperature. They behave as metals with a resistance decreasing with decreasing temperature. For the first two samples T_c is the same but it increases with the treatment temperature for the other samples (Fig. 2). Finally the increase of T_c is very clear for treatment temperatures increasing from about 900° to 950 °C. The standard a.c. four probe technique is employed to measure the resistivity. The value of alternative current is 100 μA, and the frequency is 77 Hz. For electron microscopy and microanalysis we choose a small piece of each measured sample, crush it in pure alcohol, and mount it on a holey carbon grid. A JEOL 2000 FX with high angle EDX detector was used for observation. The electron beam probe was about 100 nm diameter for composition analysis and 50 nm diameter for microdiffraction. The method used for EDX analysis, diffraction and imaging was the technique developed by one of us previously [18]. This procedure guarantees that all data (composition, diffraction and image) are taken from the same area. Peaks located at 1.81, 2.42, 3.69, 7.47, 8.04, 10.84, 13.02 and 14.14 keV correspond to characteristic X-ray lines of $Sr_{L\alpha}$, $Bi_{M\alpha}$, $Ca_{k\alpha}$, $Ni_{K\alpha}$, $Cu_{K\alpha}$, $Bi_{L\alpha}$, $Bi_{L\gamma}$, and $Sr_{k\alpha}$ respectively. The Cu peak is not considered (though it is better to use Ni grids) because some intensity comes from the sample holder. According to the thin film approximation [19], if X-ray absorption and fluorescence effects can be neglected (which is

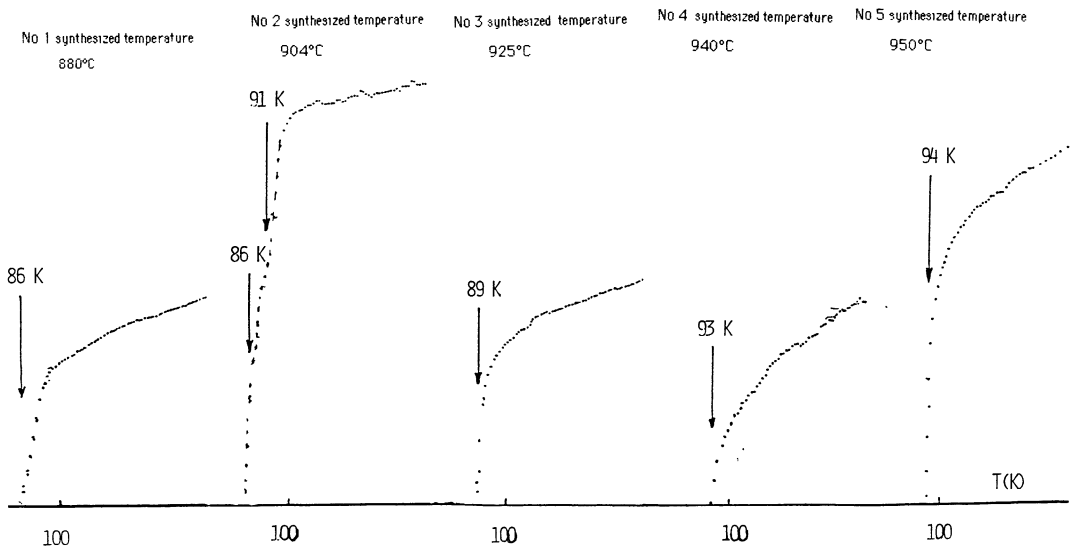

Fig. 2. — Resistivity, in arbitrary units, *versus* temperature for different samples with the normal composition (2212) for different treatment temperatures. T_c clearly increases (from No. 2 to No. 5) with the treatment temperature from about 900 °C to 950 °C.

obviously not perfectly true, but approximately true for very thin films), the concentration ratio [A]/[B] in weight percent of the two elements A and B, is proportional to the observed X-ray intensity ratios $\mathbf{I}_A/\mathbf{I}_B$, and is represented by the following expression : $[A]/[B] = k_{AB}\,\mathbf{I}_A/\mathbf{I}_B$, where k_{AB} is an experimental parameter which was determined from standard specimens with known compositions of Bi_2CuO_4, Ca_2CuO_3 and $VBaSrCu_3O_y$. The experimental errors, in relative values, can be estimated to 5 % on the standard compounds and to 10 % in the superconductor. It should be pointed out that the absolute error on the quantitative compositions is probably higher and difficult to estimate. So we will only consider relative values as significant. Therefore we chose one position where the ratios are almost Sr/Ca = 2 and Bi/Sr = 1 as the reference, then move the electron probe to other positions to get these ratios and the microdiffractions. At least 10 positions on each sample have been measurated and the data is an average value. It is interesting to note that in the Bi-Sr-Ca-Cu-O system two types of superconductors have been related to different values of the

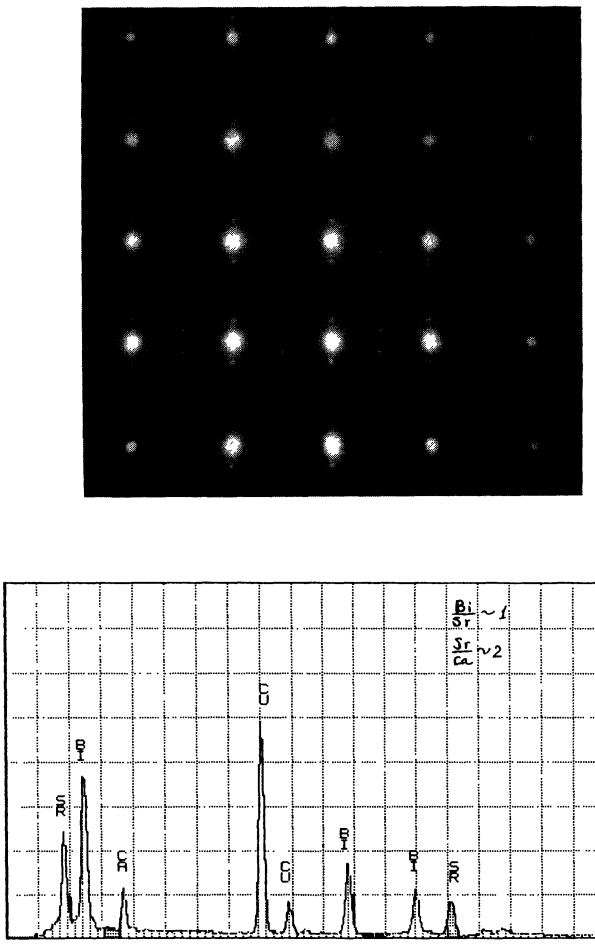

Fig. 3. — Diffraction patterns and EDX spectra of No.s 1, 4, and 5 samples the resistivity of which is given (Fig. 1).

a) Sample No. 5 : $\mathbf{q}^* = 2\,\mathbf{b}^*/4.80$; M_1 type modulation ; [Bi]/[Sr] = 1, [Sr]/[Ca] = 2, Treatment temperature 950 °C, T_c = 94 K.

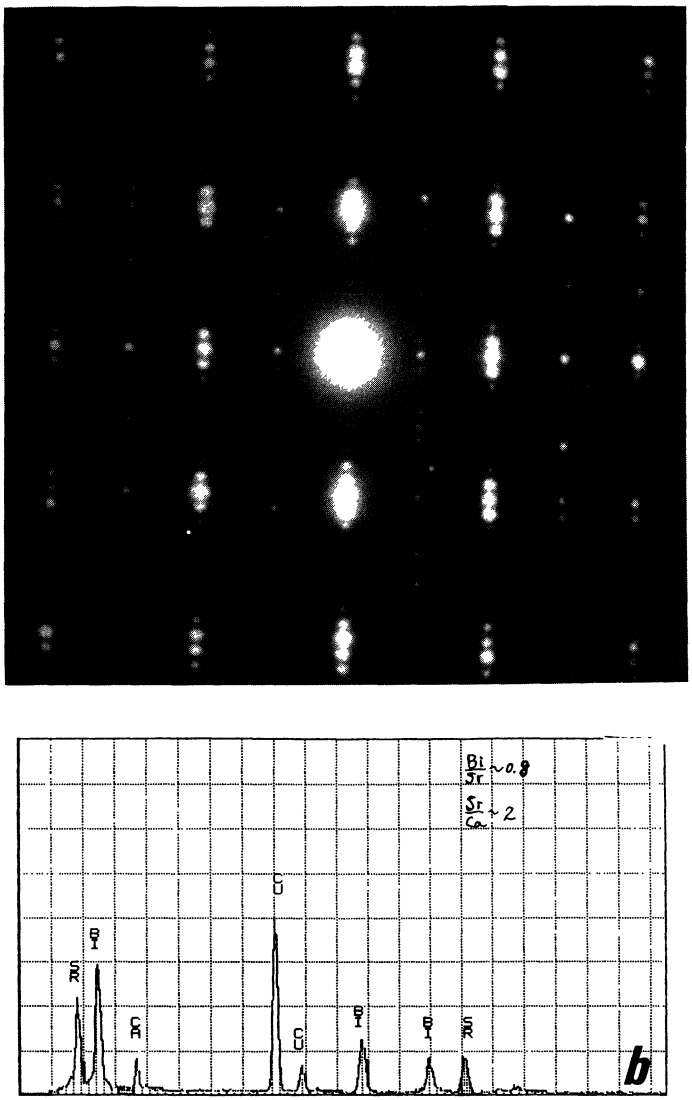

b) Sample No. 4 : $\mathbf{q}^* = 2\,\mathbf{b}^*/9.69$; M_3 type modulation ; [Bi]/[Sr] = 0.8, [Sr]/[Ca] = 2 ; Treatment temperature 940 °C ; T_c = 93 K.

[Ca]/[Sr] ratios [20]. Therefore we focused our attention on the variations of the [Bi]/[Sr] and [Ca]/[Sr] ratios and we have related them to the diffraction patterns of the same area.

Figure 2 shows resistivity *versus* temperature for samples of different heat treatment temperatures. The T_c temperature is 86 K for 880 °C (No. 1) ; 86-91 K for 904 °C (No. 2) ; 89 K for 925 °C (No. 3) ; 93 K for 940 °C (No. 4) ; 94 K for 950 °C (No. 5) respectively. Different crystals obtained in the same conditions always give the same T_c value at the precision of the experiment (± 0.5 K). The T_c value is clearly increasing with the heat treatment temperature.

Figure 3 shows the corresponding microdiffractions in the [001] zone with EDX spectra for No. 1 (Fig. 3c), No. 4 (Fig. 3b), No. 5 (Fig. 3a) samples. The [Bi]/[Sr] and [Ca]/[Sr] ratios

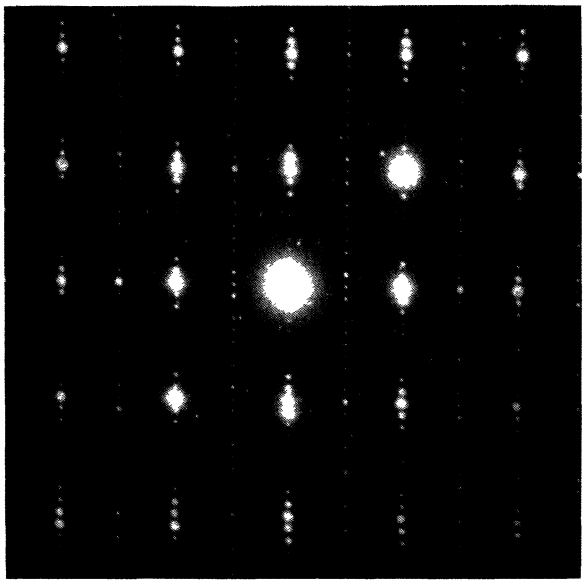

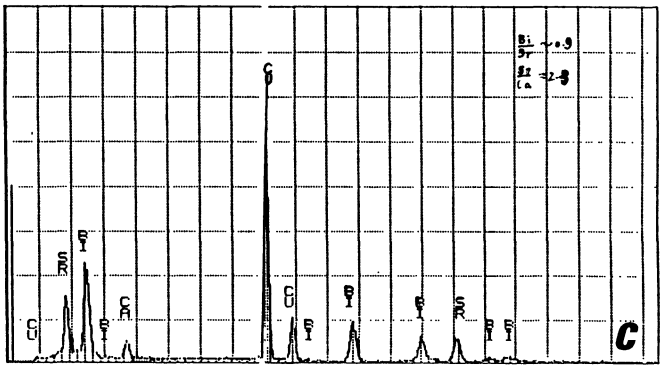

c) Sample No. 1 : $\mathbf{q}^* = 2\,\mathbf{b}^*/9.89$; M_3 type modulation ; [Bi]/[Sr] = 0.9, [Sr]/[Ca] = 2.4 ; Treatment temperature 880 °C.

have been indicated on the spectra. From these diffraction patterns we can obtain the $2\,b^*/q^*$ values (by measuring the ratio of perovskite to satellite spots distances). In table II, heat treatment temperatures, T_c values, composition ratios, $2\,b^*/q^*$ values and the type of the modulations have been listed. It is interesting to point out that the [Bi]/[Sr] ratios for the No. 1 and No. 4 samples are less than one. The difference in the composition for the different samples is clearly established from the experimental results, but local differences also exist in each sample and the value given in table II is an average value. Nevertheless it seems that the observed differences can be related to the different heat treatment temperatures.

In order to clarify the relationships between the modulations, we sketch the experimental data in a chart, giving relations between q^* values, treatment temperatures, [Ca]/[Sr] ratios and $m = 1, 2$ satellite intensities (Fig. 4). The following points can be extracted from this chart and from table II.

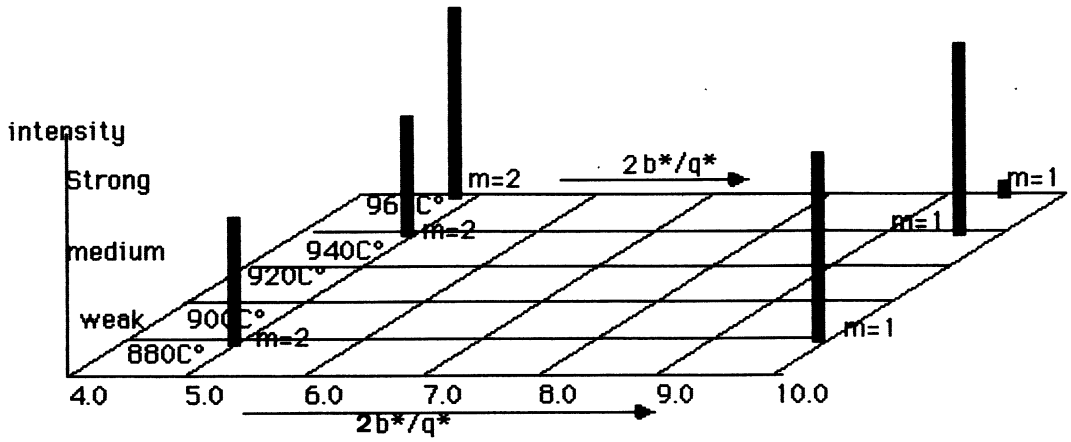

Fig. 4. — Chart of the relationship between the intensity of m_1 and m_2 satellites and **B**, **C**, **D** type reflections, with the samples treatment temperatures.

Table II. — *Comparison of heat treatment temperatures, T_c values, composition ratios, $2\,b^*/q^*$ values and modulation types for our single crystal samples.*

Sample	No. 1	2	3	4	5
Heat treatment temperature	880 °C	904 °C	925 °C	940 °C	950 °C
T_c values	86 K	86-91 K	89 K	93 K	94 K
Composition ratio					
[Bi]/[Sr]	0.9			0.8	1.0
[Sr]/[Ca]	2.3			2.0	2.0
$2\,b^*/q^*$ values	9.89			9.69	4.80
Type de modulation	M_3			M_3	M_1

1) The lowest T_c value is obtained for the lowest treatment temperature.

2) An incommensurate phase, with an approximately sinusoidal modulation ($2\,b^*/q^* = 4.80$) and M_1 type, occurs in the normal (2212) type compound for the highest treatment temperature 950 °C. This phase has been previously observed by many authors [2, 5, 6, 7, 8, 9, 12]. An approximately sinusoidal modulation wave is characteristic of a stable incommensurate phase far from a possible lock-in transition [21].

3) When one reduces the heat treatment temperatures from 950 °C the modulation is modified from the approximately sinusoidal modulation to an unsinusoidal modulation with several harmonic satellites (Fig. 5). The system turns to the M_3 type modulation. The $2\,b^*/q^*$ value (9.89) is close to an integer value (10).

4) The approximately sinusoidal modulation with $2\,b^*/q^* = 4.80$ seems to correspond to a standard composition ratio of the (2212) phase. The modulation with harmonic satellites has some composition deviation from the standard (2212) phase.

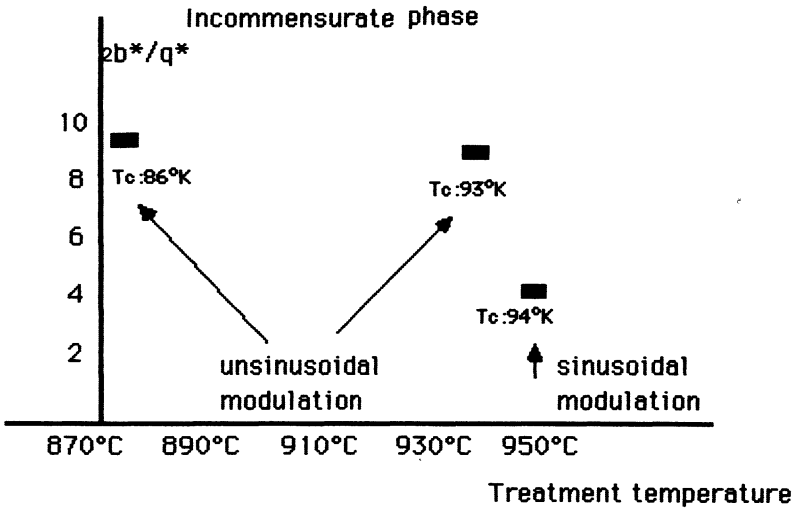

Fig. 5. — Relationship between the heat treatment temperature and $2\,b^*/q^*$ values for No. 1 ($T_c = 86$ K), No. 4 ($T_c = 93$ K), No. 5 ($T_c = 94$ K) samples.

5) For the incommensurate phases, having approximately sinusoidal modulation wave, **D** spots are always very very weak or invisible ; **B** spots are weak ; **C** spots are very weak. For the incommensurate phase in the unsinusoidal region the **B**, **C** spots have medium intensity, and the **D** spots are visible or medium. This phenomenon can be related to the different modulations. When the modulation is approximately sinusoidal the superstructure spots of the perovskite sublattice (**B** and **D**) are weaker, this means that in this case any kind of ordering process should be especially weak and this is stronger in the modulation direction.

Discussion.

The existence of three types of diffraction patterns in the [001] zone of perovskite sublattice might give a clue to understand what happens in the structure. The **B** and **D** spots, respectively along the [110] and [1$\bar{1}$0] orientations, play the same role related to the perovskite sublattice. They correspond to a superstructure in these two directions. But their intensities can be very different. While **D** spots are always invisible or very weak, **B** spots can be of medium intensity in the M_2 type or visible in the M_3 type, and are invisible only in the M_1 type. Their difference corresponds to different ordering degree of the perovskite structure in these two directions. This fact means that the [110] and [1$\bar{1}$0] orientations do not play the same role for ordering conditions. This is probably due to the modulation because the **D** spots in the direction of the modulation are always nearly invisible. The important differences in the intensity of the **B** spots, related to differences in the ordering degree might also be related to the modulation wave in the [1$\bar{1}$0] orientation, though the situation is not as clear as in the other direction.

Different models have been given for the origin of the modulation. A discussion of this origin is given by [22]. It could be due i) to extra oxygen in the BiO layer [2] ii) to Sr vacancies [23] iii) to different kinds of possible substitution [7, 8]. The obvious variation of intensity of the satellite spots between M_1, M_2 and M_3 types implies that the atomic

displacements in the $[1\bar{1}0]$ direction of the perovskite sublattice can be different, which could be related to the important variation of composition ratios of Sr and Ca cations that we have observed.

From the cell parameters, it is likely that the structure of the Bi-Sr-Ca-Cu-O compounds with $c \approx 30$ Å is closely related to that of $Bi_4Ti_3O_{12}$ (orthorhombic structure with $a = 5.448$ Å, $b = 5.411$ Å, $c = 32.83$ Å [24]) which has the structure formula $(Bi_2O_2)^{2+}(A_{n-1}B_nO_{3n+1})^{2-}$ (the general chemical formula being : $(Bi_2A_{m-2})B_{m-1}O_{3m}$, with $n = m - 1$). These compounds consist of a regular intergrowth of the perovskite structure with $\mathbf{Bi_2O_2}$ sheets consisting of BiO_4 square pyramids sharing edges [25], as indicated Fig. 6 [24]. Between the $\mathbf{Bi_2O_2}$ sheets there are n layers of corner-shared octahedra and $(n-1)$ layers of perovskite-type A cations in the twelve-coordinated interstices [25]. In the Bi-Sr-Ca-Cu-O compounds, B sites are occupied by Sr or Ca and $n = 3$ for the (2212) phase. The A positions are occupied by Cu cations. Radii of the 6-coordination Sr and Ca cations in oxides : r_{Sr} and r_{Ca} respectively are : 1.16 Å and 1.00 Å [26], the relative difference $|r_{Sr} - r_{Ca}|/r_{Sr}$ is 13.6 %. This value indicates a great tendency of ordering for Sr and Ca cations in the perovskite layers, it could be at the origin of the ordering in the [110] direction. Because of the modulation this ordering may be destroyed in the $[1\bar{1}0]$ direction. Matsui, *et al.*, recently published a very clear high resolution image of the modulation [7, 8]. They indicate that the lattice distortion is mainly located in Bi-concentrated bands. This might be attributed to some substitution of Bi with Sr or Ca atoms, related to a lack of ordering in one direction.

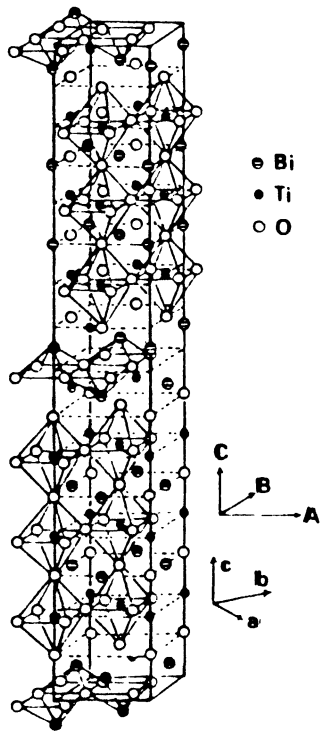

Fig. 6. — Structure of the $Bi_4Ti_3O_{12}$ compound (from [24]). The perovskite crystallographic axes are indicated by small letters on the figure. The directions of the crystallographic axes are indicated by capital letters.

Conclusion.

The experimental data of microanalysis and microdiffraction of a single region of different samples subject to different high temperatures with normal compositions (2212), yield the following points of interest :

1) An approximately sinusoidal modulation with $2\,b^*/q^* = 4.80$ exists in the single crystal with standard composition of (2212) phase and T_c values 94 K. This incommensurate phase was obtained by heat treatment temperature up to 950 °C.

2) When the heat treatment temperature is decreased from the 950 °C, the modulation is modified from the sinusoidal to the unsinusoidal region with $2\,b^*/q^*$ close to 10, but not an integer. The composition ratio of the Sr, Ca, and Bi cations is then deviated from the standard (2212) phase and the T_c value is reduced.

Acknowlegments.

Authors are gratefull to the CRMC2 for the use of 2 000 FX Jeol electron microscope, and to Mr. S. Nitshe for his help.

References

[1] MAEDA Y., TANAKA M., FUKUTOMI M., ASANO T., *Jap. Journ. Appl. Phys.* **27** (1988) L209.
[2] VAN TENDELOO G., ZANDBERGEN H. W., VAN LANDUYT J., AMELINCKX S., *Appl. Phys.* **A 46** (1988) 153.
[3] SUBBANNA G. N., GANAPATHI L., RAO C. N. R., JEFFERSON D. A., *Mat. Res. Bul.* **22** (1987) 205.
[4] VAN TENDELOO G., ZANDBERGEN H. W., AMELINCKX S., *Solid State Commun.* **66** (1988) 927.
[5] BANDO Y., KIJIMA T., KITAMI Y., TANAKA J., IZUMI F., YOKOYAMA M., *Jap. Journ. Appl. Phys.* **27** (1988) 358.
[6] KIJIMA T., TANAKA J., BANDO Y., ONODA M., IZUMI F., *Jap. Journ. Appl. Phys.* **27** (1988) L369.
[7] MATSUI Y., MAEDA H., TANAKA Y., HORIUCHI S., *Jap. Journ. Appl. Phys.* **27** (1988) L361.
[8] MATSUI Y., MAEDA H., TANAKA V., HORIUCHI S., *Jap. Journ. Appl. Phys.* **27** (1988) L372.
[9] HIRAGA K., HIRABATASHI M., KIKUCHI M., SYONO Y., *Jap. Journ. Appl. Phys.* **27** (1988) L573.
[10] TAKAYAMA-MUROMACHI E., UCHIDA Y., ONO A., IZUMI F., ONODA M., MATSUI Y., KOSUDA K., TAKEKAWA S., KATO K., *Jap. Journ. Appl. Phys.* **27** (1988) L365.
[11] KIJIMA N., ENDO H., TSUCHIYA J., SUMIYAMA A., MIZUNO M., OGURI Y., *Jap. Journ. Appl. Phys.* **27** (1988) L821.
[12] ONODA M., YAMAMOTO A., TAKAYAMA-MUROMACHI E., TAKEKAWA S., *Jap. Journ. Appl. Phys.* **27** (1988) L833.
[13] TALLON J. L., BUCKLEY R. G., GILBERD P. W., PRESLAND M. R., BROWN I. W. M., BOWDEN M. E., CHRISTAIN L. A., GOGUEL R., *Nature* **333** (1988) 153.
[14] SUBRAMANIAN M. A., TORARDI C. C., CALABRESSE J. R., GOPALAKRISHNAN J., MORRISSEY K. J., ASKEW, T. R., FLIPPPEN R. B., CHOWDHRY U., SLEIGHT A. W., *Science* **26** (1988) 1015.
[15] TARASCON J. M., LE PAGE Y., BARBOUX P., BAGLEY B. G., GREENE L. H., MCKINNON W. R., HULL G. M., GIROUD M., HWANG D. M., *Phys. Rev. B* **37** (1988) 9382.
[16] GAO L., HUANG Z. L., MENG R. L., HOR P. H., BECHTOLD J., SUN Y. Y., CHU C. W., SHENG Z. Z., HERMANN A. M., *Nature* **332** (1988) 623.
[17] KANG Z. C., BOULESTEIX C., MORIN D., PIERRE L., submited to *Phys. Solid. State.*
[18] KANG Z. C., *J. Electron Microscopy technique* **4** (1986) 343.
[19] CLIFF G., LORIMER G. W., *J. Microsc.* **103** (1975) 203.

[20] ADACHI S., INOUE O., KAWASHIMA S., *Jap. Journ. Appl. Phys.* **27** (1988) L344.
[21] JANSSEN T., Modern problems in condensed matter sciences, Vol. 14.1, p. 70 (1986).
[22] ZANDBERGEN H. W., GROEN W. A., MIJLHOFF F. C., VAN TENDELOO G. and AMELINCKX S., *Physica C* **156** (1988) 325.
[23] GAI P. L. and DAY P., *Physica C* **152** (1988) 335.
[24] DORRIAN J. F. NEWNHAM R. E., SMITH D. K., KAY M. I., *Ferroelectrics* **3** (1971) 17.
[25] GOODENOUGH J. B., LONGO J. M., « Landolt-Bornstein Tabellen », New Series III/4a, p. 146, Springer-Verlag, Berlin (1970).
[26] SHANNON R. D., PREWITT C. T., *Acta Crystallogr. B* **25** (1969) 925.